membranes

MDPI

Review

Heavy Atom Detergent/Lipid Combined X-ray Crystallography for Elucidating the Structure-Function Relationships of Membrane Proteins

Shinya Hanashima [1], Takanori Nakane [2,†] and Eiichi Mizohata [3,4,*]

1 Department of Chemistry, Graduate School of Science, Osaka University, 1-1 Machikaneyama, Toyonaka 563-0043, Japan; hanashimas13@chem.sci.osaka-u.ac.jp
2 Department of Biological Sciences, Graduate School of Science, The University of Tokyo, Tokyo 113-0033, Japan; tnakane@mrc-lmb.cam.ac.uk
3 Department of Applied Chemistry, Graduate School of Engineering, Osaka University, 2-1 Yamadaoka, Suita 565-0871, Japan
4 Japan Science and Technology Agency, PRESTO, Kawaguchi 332-0012, Japan
* Correspondence: mizohata@chem.eng.osaka-u.ac.jp; Tel.: +81-6-6879-7410; Fax: +81-6-6879-7409
† Present address: MRC Laboratory of Molecular Biology, Cambridge CB2 0QH, UK.

Abstract: Membrane proteins reside in the lipid bilayer of biomembranes and the structure and function of these proteins are closely related to their interactions with lipid molecules. Structural analyses of interactions between membrane proteins and lipids or detergents that constitute biological or artificial model membranes are important for understanding the functions and physicochemical properties of membrane proteins and biomembranes. Determination of membrane protein structures is much more difficult when compared with that of soluble proteins, but the development of various new technologies has accelerated the elucidation of the structure-function relationship of membrane proteins. This review summarizes the development of heavy atom derivative detergents and lipids that can be used for structural analysis of membrane proteins and their interactions with detergents/lipids, including their application with X-ray free-electron laser crystallography.

Keywords: membrane protein; lipid; detergent; chemical synthesis; X-ray free-electron laser (XFEL); serial femtosecond crystallography (SFX); structure-function relationship

Citation: Hanashima, S.; Nakane, T.; Mizohata, E. Heavy Atom Detergent/Lipid Combined X-ray Crystallography for Elucidating the Structure-Function Relationships of Membrane Proteins. *Membranes* **2021**, *11*, 823. https://doi.org/10.3390/membranes11110823

Academic Editors: Akira Naito and Izuru Kawamura

Received: 13 September 2021
Accepted: 23 October 2021
Published: 27 October 2021

1. Introduction

All cellular organisms have biomembranes composed of lipids, which form a boundary between the cell cytoplasm and the surrounding extracellular environment and organize complex structures inside the cell to construct cellular organelles [1]. Membrane proteins localize in the lipid bilayer of biomembranes and play a variety of important functions such as transport of various substances between the inside and outside of the cell, signal transduction, energy synthesis, and cell adhesion. In particular, membrane proteins associated with human diseases are attracting considerable attention as drug targets and are actively studied. Compounds that bind to membrane proteins and inhibit or promote their functions are being explored as drug candidates, and membrane proteins overexpressed on the surface of certain cancer cells are targets for the development of antibody drugs [2–5]. Thus, elucidation of the structure and function of membrane proteins including their interactions with lipids at the molecular level is essential both from the perspective of basic science to understand the mechanisms of life and from the perspective of medical applications. However, the progress of membrane protein research has lagged behind that of water-soluble proteins because of the difficulties associated with isolating hydrophobic membrane proteins in sufficient quantity and quality for analysis. In the field of structural biology, only about 6000 of the approximately 180,000 structural coordinates registered in the Protein Data Bank (PDB) are those of membrane proteins.

Nonetheless, advances in research technology have accelerated the study of membrane protein structures. With the continuous development of genetic engineering, expressing high levels of stable membrane proteins as recombinant proteins and purifying them with a sufficient yield has gradually become possible. High-speed atomic force microscopy has made it possible to image motion during functioning with nanometer-order spatial resolution without destroying the structure of biological samples [6]. Cryo-electron microscopy has undergone remarkable technological improvements over the last decade, enabling structural analysis of membrane proteins and their complexes with near-atomic resolution without requiring crystal preparation [7]. Most attempts to visualize the three-dimensional structure of membrane proteins and their interactions with lipids/detergents at near-atomic resolution or better have been made using X-ray crystallography. Advancing synchrotron radiation facilities and beamline technologies have facilitated the determination of crystal structures of membrane proteins. This trend will continue with the development of fourth-generation synchrotron radiation sources, including X-ray free-electron laser (XFEL) facilities [8].

Solving new structures by X-ray crystallography requires both intensities and phases of structure factors of diffracted X-ray waves; however, measured diffraction patterns only give intensities (so-called "phase problem"). Therefore, experimental (de novo) phase determination methods including single or multiple heavy-atom isomorphous replacement (SIR or MIR), single- or multi-wavelength anomalous diffraction (SAD or MAD) or the combination of SIR or MIR with anomalous scattering (SIRAS or MIRAS) must be applied to solve the phase problem. Isomorphous replacement methods use the difference in reflection intensities between the native crystal and the heavy atom-labeled derivative crystal to determine the phases, whereas the anomalous diffraction method uses anomalous differences between Bijvoet pairs [9]. Both methods require accurate measurement of small intensity differences. However, expressing selenomethionine-labeled recombinant proteins is time-consuming and costly, and even if the native crystals are soaked in a heavy-atom solution, the heavy atoms often do not bind to the protein or the crystallinity easily collapses, resulting in loss of diffraction ability. Thus, the development of heavy atom labeled protein ligands is needed that bind various membrane proteins and facilitate drawing electron density maps efficiently from X-ray diffraction data to reveal three-dimensional structures.

In this review, we summarize the development and use of heavy atom derivative detergents/lipids that can be used to analyze interactions between membrane proteins and detergents/lipids and to determine the structure of membrane proteins. We also discuss the potential of combining recently developed XFEL crystallography with heavy atom detergents/lipids to understand the structure-function relationship of membrane proteins and their interactions with detergents/lipids.

2. Heavy Atom Labeled Protein Ligands

Typical de novo methods to determine crystallographic phases involve heavy-atom derivatization of protein crystals. These crystals can be used for isomorphous replacement methods and anomalous diffraction methods. The period 4 to 6 elements, including lanthanides, are often used as electron-rich heavy atoms for solving phase problems when determining protein structures by X-ray crystallography. Soaking manipulation introduces heavy metal ions or heavy atom-labeled compounds into protein crystals. The successfully soaked ions or compounds in protein crystals are immobilized through interactions with functional groups of proteins mostly by ionic and dipole linkages, H-bonding, and coordination bonding [10,11]. Numerous conditions are typically screened as a rule of thumb to ensure successful crystallization of the target protein and referring to the chemistry of ionic interactions and covalent modifications is often useful for the introduction of heavy atoms into protein crystals.

Protein ligands containing heavy atom moieties have been developed to achieve two purposes. First, these ligands unveil the molecular interactions between proteins and

ligands. The strong and characteristic diffraction of heavy atoms, due to their high electron density and anomalous scattering, reveals the ligand position on the protein. Second, the ligand can be used for de novo phasing to determine the protein structure. However, careful design of the heavy atom ligand is essentially required to avoid disturbance for the protein-ligand interaction. Heavy atom-containing detergents/lipids are potentially useful for solving structures of membrane proteins because they have affinity for the hydrophobic surface of membrane proteins and can be used to determine phases.

2.1. Halogens

Protein-ligand analogs carrying a Br or I atom have been used successfully to determine X-ray protein crystal structures with de novo phasing; however, careful design of the analog structure is important because of the properties of halogen atoms. The carbon(sp^3)–halogen bond length (C–Br: 191 pm; C–I: 216 pm) is significantly longer than the corresponding carbon–carbon bond length (151 pm) [12]. Thus, careful consideration may be required when selecting protein crystallization conditions because of the bulkiness and lower bond-dissociation energy of the carbon(sp^3)–halogen bond (C–Br: 72.4 kcal/mol; C–I: 56.9 kcal/mol) [13]. Possible instability can be overcome by installing halogens on an aromatic ring because the bond-dissociation energy between a benzene carbon (Ph) and the halogen atom is higher (Ph–Br: 84 kcal/mol; Ph–I: 67 kcal/mol) than that of carbon(sp^3)–halogen bonds [13].

The high electron density and anomalous scattering from halogen atoms are used to disclose the exact atom position in crystal structures. A powerful application is to elucidate the binding of drugs to membrane proteins. For example, the anomalous scattering of Br installed on Fluoxetine (Br–Fluoxetine), the antidepressant drug named Prozac®®, clearly reported the ligand position at the fenestration of the K2P channel TREC-2, which is regulated by arachidonic acid [14]. In a similar approach, Br-labeled Memantine, a drug used for treating Alzheimer's disease, was used to accurately unveil the binding mode to the prokaryotic pentameric ligand-gated ion channel [15]. The crystal structure indicated that the Br analog blocks the extracellular entryway of the channel pore to inhibit ion passage through the channel.

Halogen labeling has also been used to determine the crystal structure of RNA molecules. RNA is a biopolymer that plays a direct role in the regulation of cellular activities through molecular interactions. Some structures of RNA have been successfully determined through de novo phasing using halogen atoms such as 5-bromouridine [16] and 5-iodouridine [17]. Nucleotides are crucial protein substrates for maintaining cellular homeostasis. ATP mimicking analogs with a halogen atom are good inhibitors of protein kinases. The affinity of protein-inhibitor binding is dependent on the number and position of halogen substitutions, which contribute to "halogen bonding" [18]. Therefore, halogen bonding is another important function of halogen atoms introduced on the protein ligand, which may enhance ligand-protein interactions and possibly modulate the orientation of the ligand [19].

Cell membrane lipids are indispensable for regulating the structure and function of membrane-related proteins. Phospholipids carrying brominated hydrocarbon chains **1** and **2** have been used to examine phase separation and domain distributions (Figure 1) [20–22]. Namely, an electron-rich Br atom selectively positioned in the middle or terminal position of a phospholipid hydrocarbon chain efficiently acts as a collisional quencher for a fluorescence group close to the Br atom. These brominated fatty acids of phospholipids are readily prepared by substituting the terminal alcohol with Br [23] or adding Br_2 to an unsaturated bond [24]. The electron-rich Br atom can be a good reporter in X-ray diffraction studies for detecting particular atomic positions in lipid tails consisting of continuous methylene and terminal methyl groups. X-ray diffraction data of a bilayer membrane composed of mono-bromo dipalmitoylphosphatidylcholine (DPPC) **1** disclosed the terminal position of the hydrocarbon chain in the membrane, where the terminus of lipid chains was substituted with a Br instead of the ω-methyl group [25]. Br mimics the size of

the ω-methyl group of the hydrocarbon chain because both have similar van der Waals radii (Br: 185 pm; CH_3: 200 pm). Bromination did not affect the transition enthalpy and cooperativity significantly; although, mono-bromo DPPC showed a significant decrease by 9 °C in the phase transition temperature. Brominated lipids were also used to determine lipid binding sites on the surface of membrane proteins in single-crystal X-ray structural studies of proteins [26]. This was achieved by discriminating between the hydrocarbon chains of lipids and those of detergents that were used to reconstitute membrane proteins into membranes. When labeling phospholipids with Br atoms, the anomalous signals from dibromo phospholipid **2** in Figure 1 and its analogs with different lipid headgroups make it easier to discriminate lipid electron densities of surrounding lipids from those of detergents and other molecules.

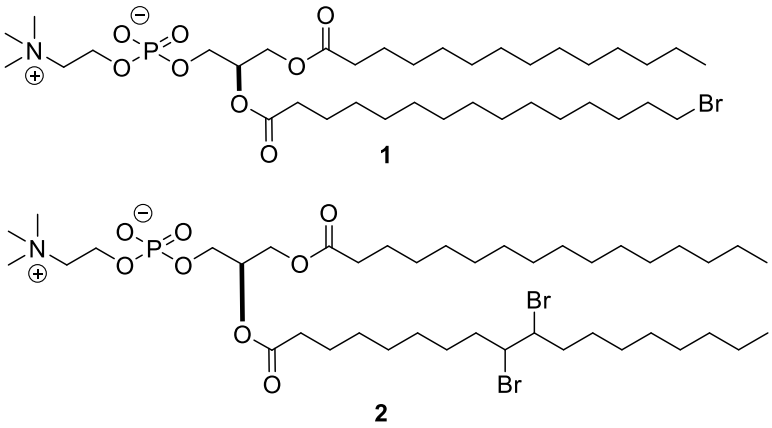

Figure 1. Structures of the bromo-phospholipids.

Brominated lipids can be used to determine lipidic ligand–protein interactions (Figure 2). Chemosensory proteins transport chemicals from air to the receptor and are associated with olfaction or taste processes. 12-Bromododecanol was used in a crystallization study as a surrogate for the hydrophobic ligand of a chemosensory protein [27]. The clear observation of three peaks in the anomalous difference electron density map revealed that three chain positions of the bromohydrocarbon occupied the large ligand cavity of the protein after major structural changes. Pheromone binding proteins are another class of odorant proteins. Similarly, iodohexadecane was used instead of the intrinsic pheromone, bombykol, to determine the conformation of the binding cavity of the insect pheromone binding protein from *Bombyx mori* [28].

We recently developed the synthetic route for ω-doubly brominated 1,2-dimyristoyl-*sn*-glycero-3-phosphocholine (Br_2-DMPC) via the tosyl intermediate (Scheme 1). Esterification of the ω-tosyl fatty acid to the two hydroxy groups on glycerophosphocholine, instead of using the ω-bromo fatty acid, successfully produced an intermediate **3** in moderate yield, and the following substitution reaction using LiBr afforded Br_2-DMPC. These brominated lipids will be used as ligands and as annular lipids in membrane protein crystallization studies.

Large membrane proteins usually consist of multiple transmembrane helices and sizable ectodomains. Therefore, labeling multiple sites of the membrane protein with heavy atoms is an approach to solve phase problems in X-ray diffraction studies. The use of appropriate detergents is often required to manipulate and crystallize membrane proteins. Detergents used for crystallization can be conveniently labeled with heavy atoms, which is suitable for de novo phasing. Accordingly, heavy atom-bearing tripod amphiphiles shown in Figure 3 were developed previously [29]; the iododetergent **4**, which solubilizes membrane proteins, is suitable for manipulating membrane proteins.

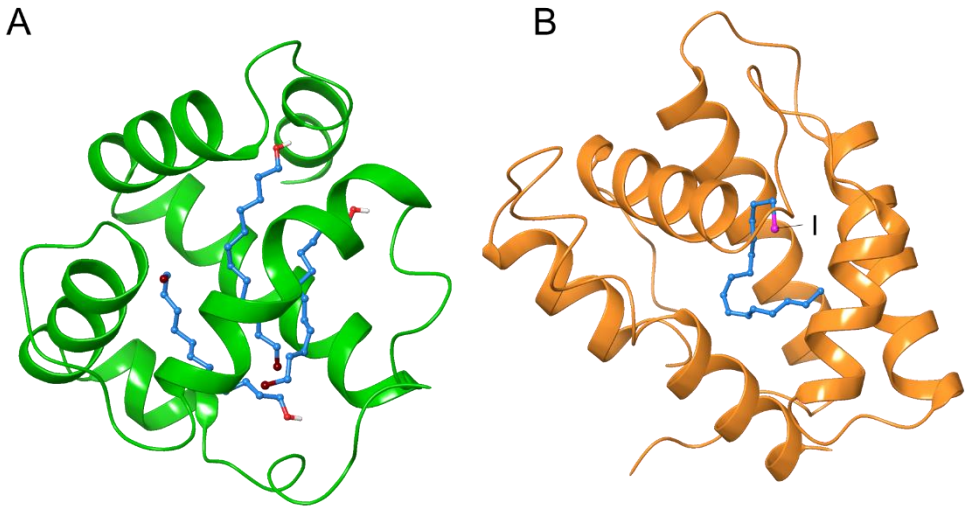

Figure 2. Crystal structures of the complex with lipidic ligands with halogen moiety. Moth chemosensory protein CSPMbraA6 with bromohydrocarbon chain (PDB ID: 1N8U) (**A**). Moth pheromone binding protein BmorPBP with iodohexadecane (PDB ID: 2P71) (**B**). Hydrocarbon chain of the ligands were shown in sky-blue, and Br and I were shown in purple and magenta, respectively.

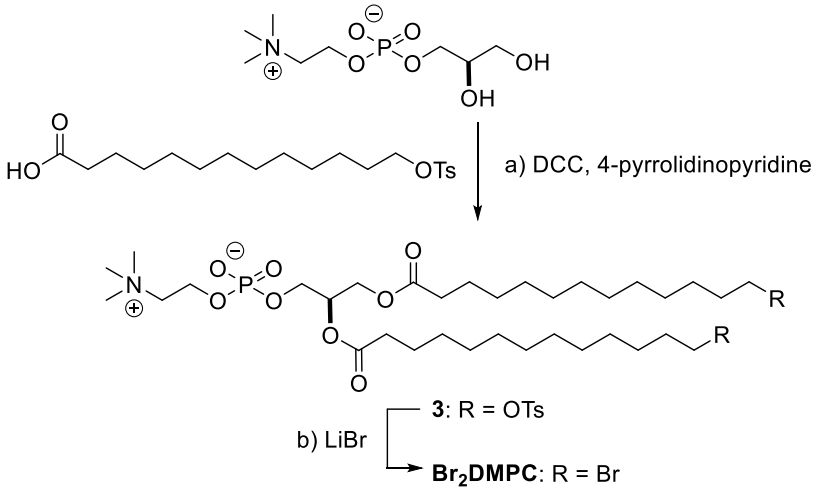

Scheme 1. Synthesis of ω-Br_2-DMPC. Synthetic procedures; (**a**) *N*,*N*′-dicyclohexylcarbodiimide (DCC), 4-pyrrolidinopyridine, CH_2Cl_2, 40%. (**b**) LiBr, acetone 41%. Ts; *p*-toluenesulfonyl group. Detail of this synthesis was described in Supplementary Materials.

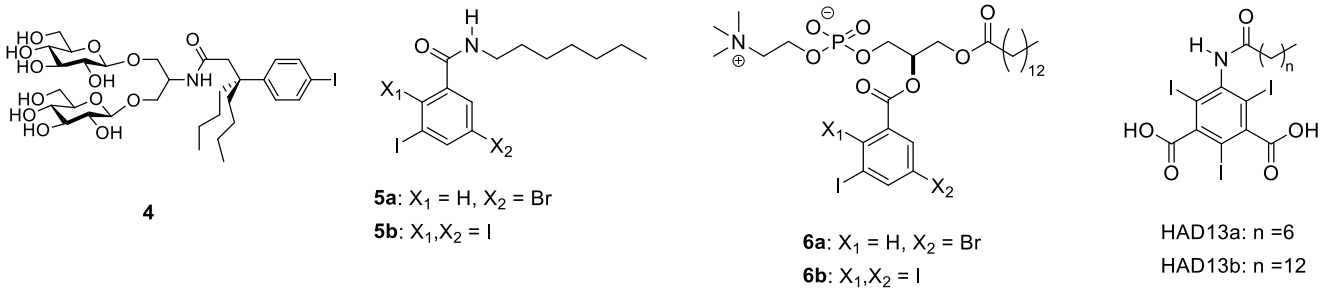

Figure 3. Lipophilic compounds and detergents bearing multiple halogen substitutions that can be used to solve the phasing problem for membrane protein structures.

We developed amphipathic compounds, phospholipid mimics and detergents bearing multiple halogen substitutions on aromatic rings for de novo phasing and revealing lipid-

protein interactions. The amphipathic properties manifested by the hydrophilic headgroups linked to the lipophilic hydrocarbon tails are essential for these molecules to mix well with bilayer membranes and interact with membrane proteins in a similar manner to intrinsic lipids (Figure 3). Furthermore, the multiple halogens arrayed on a plane of the aromatic ring assisted with the easy detection of the moiety. Commercially available benzoic acid or phthalic acid derivatives carrying multiple halogen substitutions, some of which have been used as a phasing reagent in protein crystallization [30,31], were coupled with lipophilic moieties through amidation or esterification with alkyl amine, lysophosphatidylcholine or fatty acids to give compounds **5a**, **5b**, **6a** (HAD16), **6b**, HAD13a [32], and HAD13b (see Supplementary Materials for synthetic details). Importantly, HAD13 was developed based on a successful phasing reagent 5-amino-2,4,6-triiodoisophthalic acid (I3C, or magic triangle) [30,31] for application in X-ray imaging. I3C is a common synthetic intermediate for several X-ray contrasting reagents safely used to improve the visibility of vascular structures and organs during radiographic procedures in clinical diagnostics [33,34]. I3C has been used for solving the crystal structure of more than 30 protein structures (mainly soluble proteins) in the PDB. Recently, 5-amino-2,4,6-tribromobenzene-1,3-dicarboxylic acid and tetrabromoterephthalic acid, which are bromo analogs of I3C, were successfully used as phasing reagents in the crystallization of model proteins [35,36]. Further application of I3C and other halogenated benzoates for membrane protein crystallization was achieved by improving the amphiphilicity of the halogenated benzoate by introducing an acyl chain at an amino group or coupling with a lysophospholipid. The amphiphilic nature of these compounds ensures good miscibility with phospholipids and for acting as detergents by surrounding membrane proteins. Phospholipid mimics **6a** (HAD16) and **6b** and detergents HAD13a and HAD13b were miscible in DMPC/CHAPSO bicelles (q = 2.8), which were used for crystallization of membrane proteins [37], whereas hydrophobic compounds **5a** and **5b** were shown to readily form precipitates. In practice, HAD13a was used successfully to perform de novo phasing of XFEL diffraction data obtained from membrane protein microcrystals (see details in Section 3).

2.2. Selenium

Selenium is a major heavy atom that is used to achieve de novo phasing of protein crystallographic data. Oxygen and sulfur belong to the second and third periods of the group 16 elements in the periodic table, thus being potentially substituted with a selenium element in the 4th period. Therefore, recombinant expression using selenocysteine and selenomethionine readily furnishes target proteins with heavy atom labels, which are suitable for the SAD/MAD phasing method [38]. However, care must be taken because the toxicity of selenomethionine sometimes hampers the growth of recombinant organisms used to overexpress target proteins. In addition, selenium derivatives of nucleic acids have been incorporated into DNA and RNA to solve the phase problem in MAD phasing [39].

Selenium-labeled derivatives of ligands that bind to proteins have been synthesized for protein crystallography. The selenium atom on the protein ligand is used to phase X-ray diffraction data and determine the exact atomic position of the bound ligand by using anomalous scattering, as is the case with halogen ligands. In carbohydrate chemistry, selenium-containing sugars and their derivatives have been developed as antioxidants and glycosidase inhibitors [40,41]. Although selenium is a highly toxic element, the potential of these seleno-sugars as lead compounds for therapeutic reagents has been examined [42].

Selenomethyl-*N*-acetylglucosamine (βMeSe-GlcNAc), a selenium-labeled sugar, was first used for protein crystallization to solve the phasing of data obtained on bacterial F17-G adhesin (Scheme 2) [43] because GlcNAc is a native ligand of this adhesin. The selenomethyl group was smoothly installed at the anomeric position of 1-chloro-GlcNAc. βMeSe-GlcNAc successfully mimics the native ligand because the binding constants of GlcNAc and βMeSe-GlcNAc to the adhesin are similar. Imberty and co-workers developed a selenomethyl derivative of fucose (β-MeSe-Fuc) (Scheme 2). βMeSe-Fuc was first used as a seleno-ligand for phasing when solving the crystal structures of fucose-binding lectins

derived from a plant pathogenic bacteria [44]. βMeSe-Fuc was also used to determine the co-crystal structure of other lectins AFL [45] and BC2L-C [46], which originate from the opportunistic infection-related fungus *Aspergillus fumigatus* and the bacterium *Burkholderia cenocepacia*, respectively. αMeSe-Fuc was readily synthesized by anomerization of βMeSe-Fuc with a Lewis acid [47] or glycosylation between fucosyl imidate and a selenoacetal acceptor [48]. Recently, Shimabukuro et al. successfully introduced the MeSe group at the 2–, 3–, or 4–OH position of fucose (Figure 4) and these compounds were used as ligands for a fucose binding lectin that originated from *Aspergillus oryzae* [49]. The MeSe substitution disclosed the essential hydroxy group for interaction with the lectin. Currently, the selenium atom can be incorporated into an oligosaccharide structure, which facilitates applications of seleno probes to elucidate oligosaccharide binding to proteins by not only crystallography but NMR because ^{77}Se (I = 1/2, 7.6% natural abundance) is an NMR active nucleus that gives rise to a sharp signal [50].

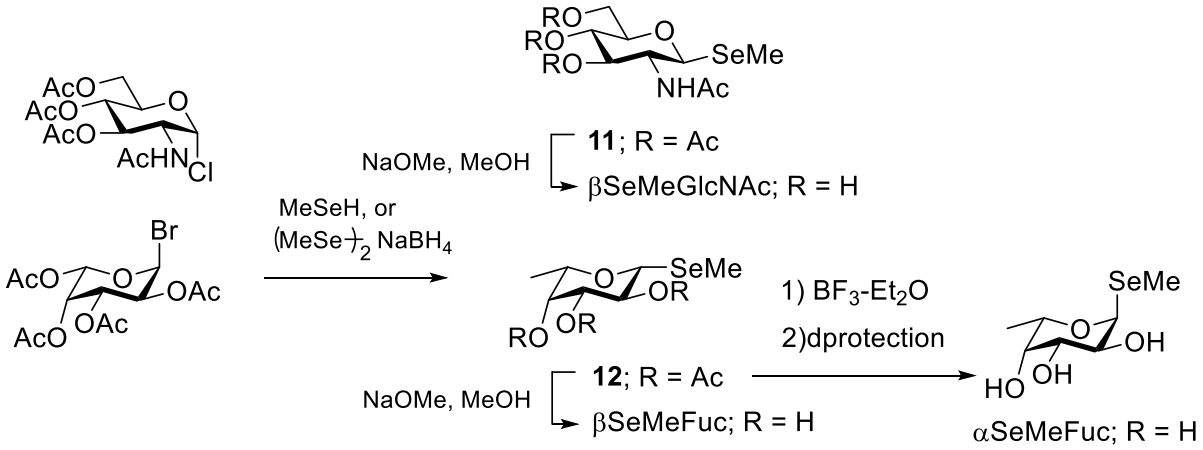

Scheme 2. Synthetic scheme of the selenoglycosides where selenium was substituted at the glycoside oxygen.

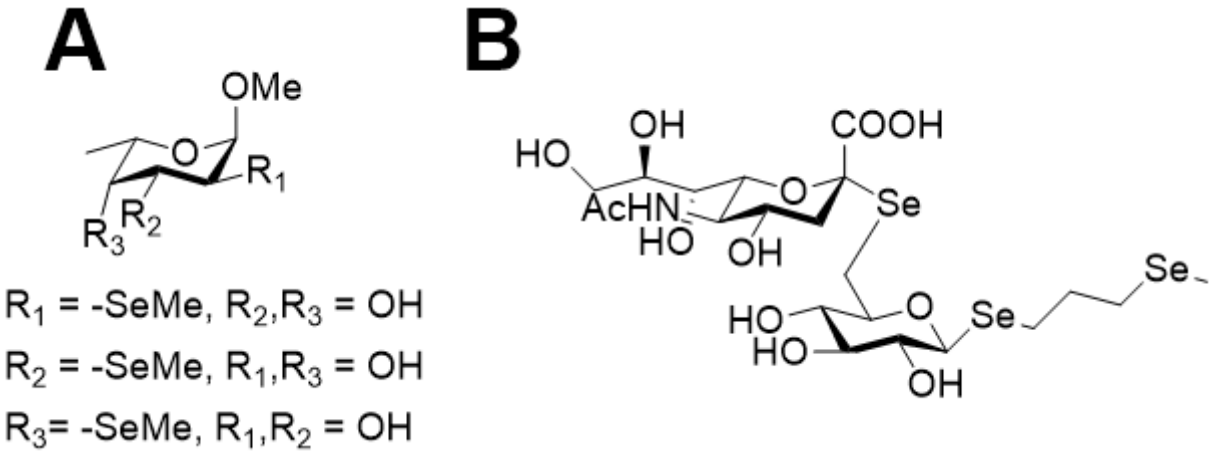

Figure 4. Fucose derivatives with selenomethyl substitutions at the 2, 3, or 4 hydroxy group (**A**) and sialylglucose derivative with three selenomethyl substitutions (**B**).

The hydrophilic sugar moieties are also used as headgroups of detergents to manipulate and crystallize membrane proteins. Detergents carrying a heavy atom can be used in membrane protein studies. Dodecyl-*β*-D-selenomaltoside (SeDDM), a heavy atom analog of dodecyl-*β*-D-maltoside (DDM), was used to achieve MAD phasing when solving the structure of leukotriene C4 synthase by X-ray crystallography (Figure 5A) [51]. Furthermore, SeDDM was used successfully as a phasing detergent to solve the structure of the prokaryotic pentameric ligand-gated ion channel [52]; however, the sugar headgroups

were poorly resolved (Figure 5B). Detergent bundles of SeDDM were clearly observed inside the pore.

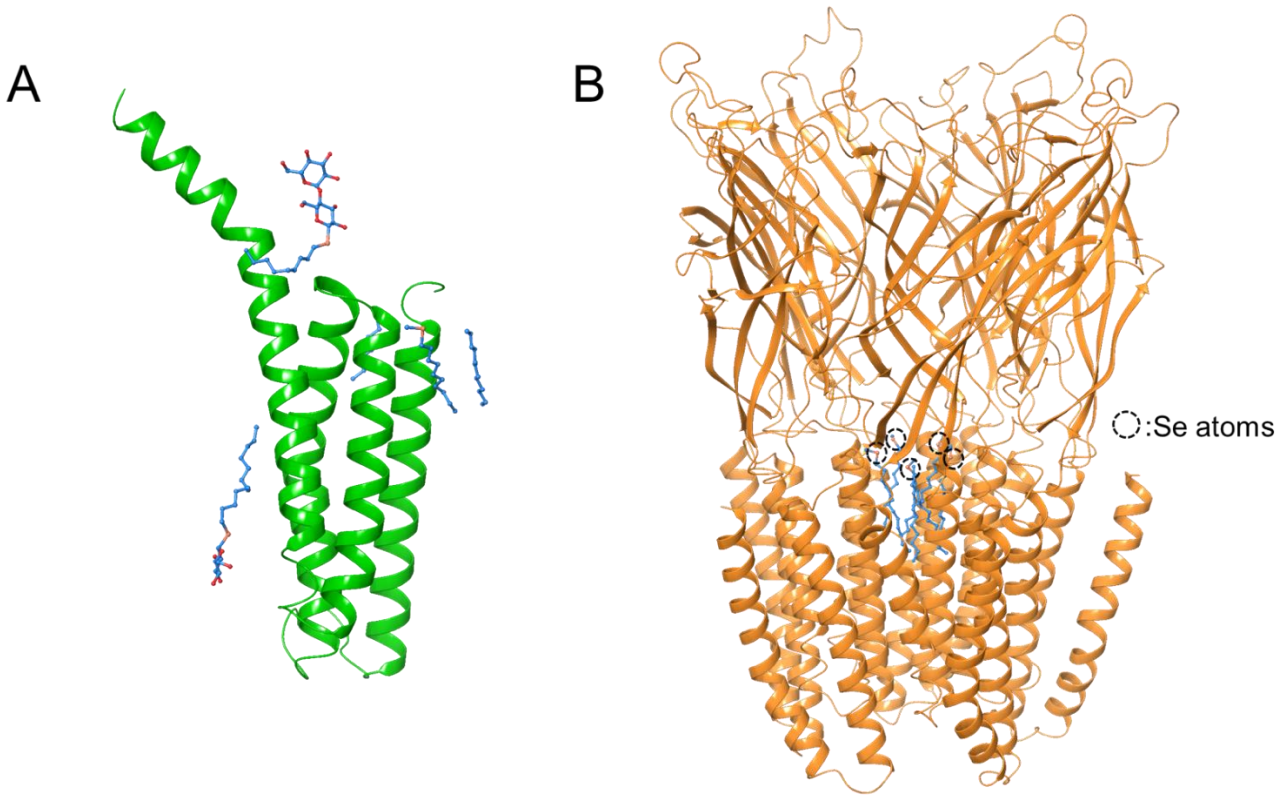

Figure 5. Crystal structures of transmembrane proteins Leukotriene C4 synthase (PDB ID: 3B29) (**A**) and pLGIC pentamer (PDB ID: 4IL4) (**B**) using SeDDM as the phasing detergent. The hydrocarbon chains of Se-DDM are shown in sky-blue.

Fatty acids are amphiphilic compounds ubiquitously present in our body. A seleno-fatty acid whose methylene group was substituted with a selenium atom was developed because their van der Waals radii are very similar (Se: 190 pm; CH_2: 200 pm). Carbon belongs to group 14 and is thus different from selenium in the periodic table. This difference results in a slightly longer bond length (C–Se: 194.5 pm; C–C: 154.0 pm) and a smaller bond angle (C–Se–C: 96.3°; C–C–C 112.6°). Thus, the distance between the two carbon atoms of a C–Se–C moiety is 289.8 pm, which is 34 pm longer than the distance of 1,3-carbon atoms in an alkane. However, this difference does not affect the conformation of the whole acyl chain significantly, except for the selenoether and its neighboring portions. Therefore, selenium can be used as a bioisostere for a methylene unit, which is particularly useful for introducing a heavy atom into the hydrophobic part of detergents and ligands. For example, Fredga and Lindgren first reported the synthesis of 4-seleno-hexadecanoic acid and 12-seleno-hexadecanoic acid, the seleno analogs of palmitic acid (Scheme 3) [53]. Two or more selenium atoms were also incorporated into a fatty acid using a similar synthetic pathway [54]. Sadek and Basmdjian incorporated radioactive ^{75}Se into fatty acid chains for imaging [55].

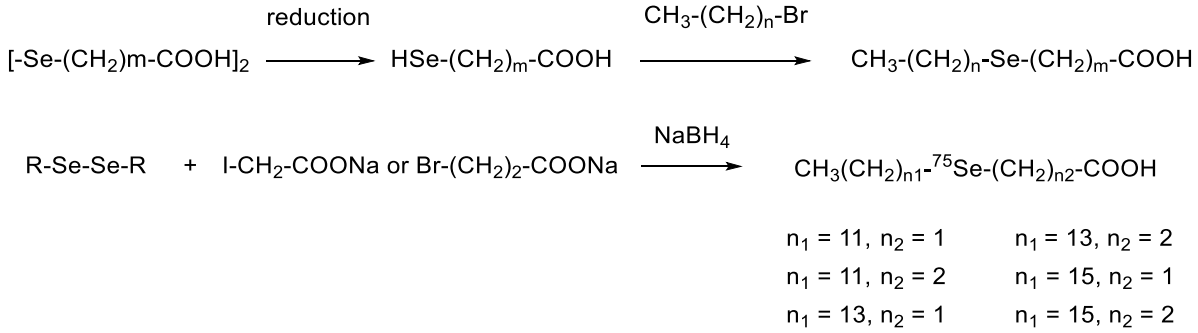

Scheme 3. Conventional synthesis of seleno-fatty acids.

Selenium is an essential trace element and a source of the antioxidant selenoproteins. Ether-type lipids bearing a selenomethyl moiety at the terminus of a hydrocarbon chain were synthesized to gain antioxidant activity [56,57]. Interestingly, seleno fatty acids were also developed as antimicrobial agents [58]. These seleno-lipid derivatives can be used to solve the phase problem in appropriate protein crystallization studies.

Lipidic ligands carrying a heavy atom moiety are also useful for revealing lipid–protein interactions, not only for phase determination but by making the heavy atom position conspicuous with the anomalous difference map. Recently, we developed a heavy atom derivative of α-galactosylceramide (α-GalCer) known as KRN7000, which activates immune responses by inducing cytokine production upon binding to the protein CD1d (Figure 6) [59]. Selenium was incorporated into the fatty acid chain of α-GalCer by substitution of a methylene group through chemical synthesis. The selenium and ω-halo derivatives were potent inducers of IFN-γ and IL-4 production in murine splenocytes. The heavy atom-modified lipid derivatives of α-GalCer were accommodated deeply in the lipid-binding cavity of CD1d.

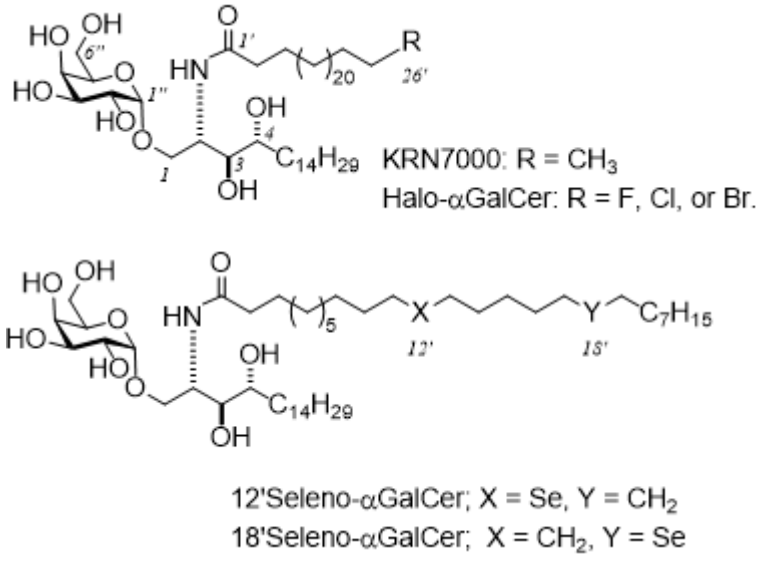

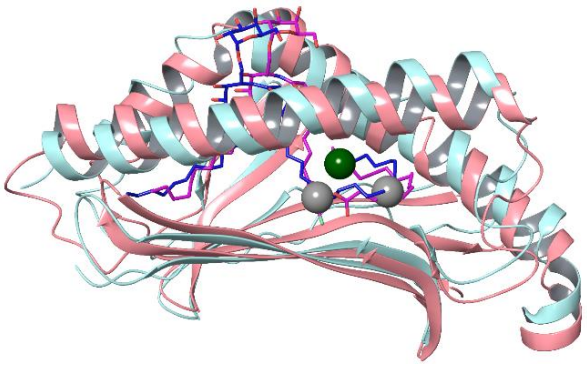

(**A**) (**B**)

Figure 6. Structures of heavy atom derivatives of α-galactosylceramide and binding model with CD1d. The chemical structures of α-GalCer derivatives with terminal halogens or selenium (**A**), and the superposed structures of murine CD1d complexed with Th1-selective ligand C8PhF (PDB ID: 3GMO; pink ribbon and purple wire) and that with KRN7000 (PDB ID: 3HE6; sky-blue ribbon and blue wire) (**B**). C26′ of KRN7000 is shown as a dark green ball and C12′/C18′ are shown with gray balls, which corresponded to halogen and selenium positions of the synthetic analogues, respectively.

3. Serial Femtosecond Crystallography (SFX)

An important recent innovation in quantum beam technology for structural biology is the emergence of XFEL. The world's first XFEL facility, LCLS [60], was built at Stanford University in the United States in 2009. In 2011, SACLA [61] was established in Japan, followed by the European XFEL [62] in Germany, PAL-XFEL [63] in Korea and SwissFEL [64] in Switzerland. Serial femtosecond crystallography (SFX) is a new data measurement technique of X-ray crystallography, which takes advantage of the ultra-high beam brilliance, femtosecond pulse duration and high spatial coherence of XFEL [65]. At SACLA, an operation mode with a wavelength range of 0.62–2.76 Å, a pulse duration of 2–10 fs, a pulse energy ~400 uJ at 10 keV, and a frequency of 30–60 Hz is available for SFX [66].

In SFX measurements, many microcrystals are ejected at random orientations from an injector and introduced into the orbit of the XFEL beam, and the diffraction image produced when a single pulse of XFEL hits a microcrystal within a femtosecond exposure time is recorded at room temperature. Because the brightness of the XFEL is typically a billion times brighter than synchrotron radiation such as SPring-8, the diffraction intensity obtained with a single XFEL pulse is comparable to the diffraction intensity of a 1-s exposure with synchrotron radiation. Diffraction images of thousands to a half-million microcrystals are collected for structural analysis. In the case of synchrotron radiation crystallography (SRX), at least milliseconds of exposure time are required for data collection, which results in radiation damage and photoreduction, a phenomenon where hydrated electrons that are generated on the order of picoseconds by the interaction of X-rays with water molecules in the crystal react with protein molecules in the crystal to break chemical bonds and reduce metal active centers [67]. Because femtosecond XFEL diffraction in SFX is completed on a shorter timescale than the process of radiation damage and photoreduction, this technique captures the damage-free structure of samples [68].

3.1. De Novo Phasing in SFX

Since the first construction of the XFEL facility in 2009, all SFX structures reported in international journals had been solved by the molecular replacement method using known structures as search models. This is because phase determination by the anomalous scattering method requires accurate measurement of small intensity differences between the reflections of the Bijvoet pairs, which is much more difficult with SFX than with the conventional SRX oscillation method. In SFX, data are collected by irradiating a large number of microcrystals of different sizes and orientations with XFEL pulses that have fluctuations in intensities and wavelength spectra. This leads to large errors in the observed diffraction intensities, and all measurements are partial reflections, making it difficult to determine the phases. In 2014, the first de novo structure determined with SFX was reported by the Gd-SAD method using a model protein lysozyme [69]. Subsequently, we reported de novo phasing of the luciferin-regenerating enzyme by the Hg-SIRAS method [70] and lysozyme by the S/Cl-SAD method [71] in 2015 and successfully determined the structure of copper-containing nitrite reductase by the Cu-SAD method in 2016 [67]. In the same year, the phase determination of BinAB by the Hg/Gd/I-MIRAS method [72] and streptavidin by the Se-SAD method [73] were reported. Thus, successful cases of de novo phasing by SFX were reported. However, these data analyses are all from water-soluble proteins and required tens or hundreds of thousands of high-resolution diffraction images of 1.7–2.3-Å resolution. Therefore, the authors took on the challenge of developing an efficient method for the phase determination of membrane proteins by SFX.

3.2. De Novo Phasing with the HAD13a Detergent

In general, the diffraction quality of membrane protein crystals is lower when compared with that of water-soluble proteins. This is also true for SFX using the most brilliant XFEL light source available today. In the experimental phasing method of SRX, heavy atoms such as Se, Hg, Au, and Pt, which have absorption edges around 1.000 Å, have been selected frequently and used to derivatize relatively large crystals (50–200 μm). This is

because, in most cases, the beamlines used for X-ray crystallography of biological macromolecules are optimized for wavelengths around this range. In contrast, because SFX uses microcrystals (1–50 μm), X-ray beams with longer wavelengths are often selected to obtain larger diffraction signals. We selected iodine, which has an excellent anomalous scattering effect at longer wavelengths (f'' = 8.6e at 1.771 Å). HAD13a was synthesized by attaching a hydrophobic alkyl chain (caprylic acid) to I3C to give HAD13a affinity toward hydrophobic surfaces of membrane proteins [32]. HAD13a has detergent properties (CMC: 4.6 mM) and was used to label membrane proteins with heavy atoms by simply mixing it with microcrystals of bacteriorhodopsin crystallized by the bicelle method or G protein-coupled A2a adenosine receptor (A2A GPCR) obtained by the LCP method (Figure 7). The HAD13a-labeled bacteriorhodopsin was successfully phase-determined by SAD, SIR, and SIRAS methods using iodine atoms. For phase determination by the SAD method, 23,000 indexed diffraction images and a resolution of 2.1 Å were required. In contrast, in the SIRAS method with the addition of native crystal data, reflections up to a resolution of 3.3 Å were sufficient for phasing, and when the resolution was extended, only 7000 (4000 derivative and 3000 native) indexed images were required to determine the phase. This indicates that the SIRAS method is more powerful than the SAD method for efficient de novo phasing in SFX. At a similar time as our study, Batyuk et al. succeeded in determining A2A GPCR by the S-SAD method, which required 500,000 images and obtained a resolution of 2.5 Å [74].

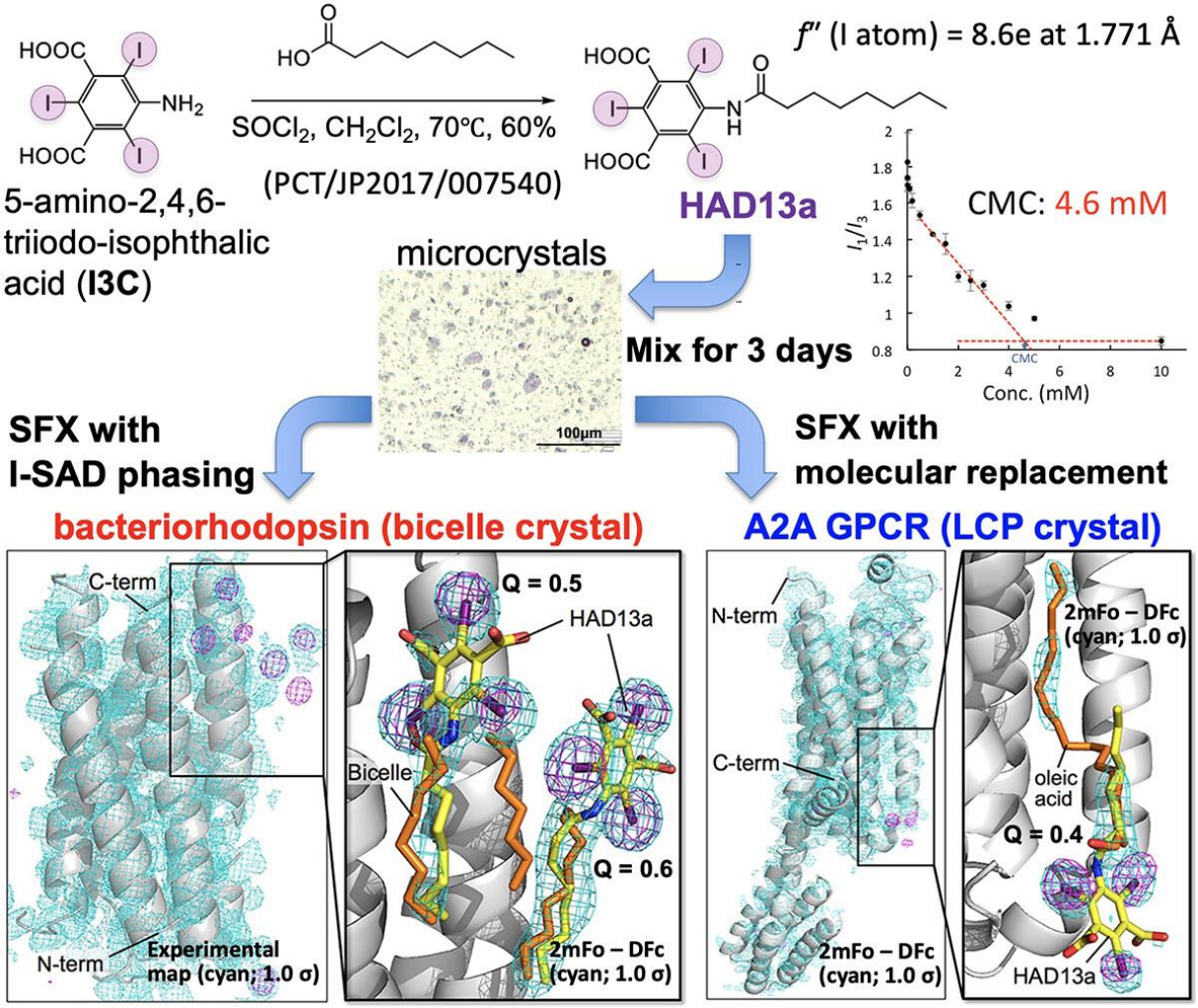

Figure 7. Serial femtosecond crystallography (SFX) of membrane proteins that have interacted with iododetergent, HAD13a. Figure reproduced with modification from Ref. [32].

3.3. Binding of the HAD16 Lipid to a Membrane Protein

HAD16 was synthesized by modifying the aromatic head group of HAD16H with multiple heavy-atom halogen groups to furnish a hydrophobic alkyl tail (Scheme 4, Supplementary Materials Section S6). The structural properties of HAD16 mimic a phosphatidylcholine structure. HAD16 can be used as a tool for analyzing lipid-membrane protein interactions. Microcrystals of bacteriorhodopsin obtained by the bicelle method were mixed with HAD16 and then SFX data were collected at SACLA (Supplementary Materials Section S7). We tried de novo phasing the HAD16 dataset. Although two heavy atom sites were located by the SIR, SIRAS or SAD method, auto-tracing was not possible even with all 18,069 lattices obtained. This is most likely because of the smaller isomorphous and anomalous signal from HAD16, which contains only one I atom and one Br atom per molecule instead of three I atoms in HAD13a, as well as only one HAD16 molecule in the asymmetric unit when compared with two HAD13a molecules.

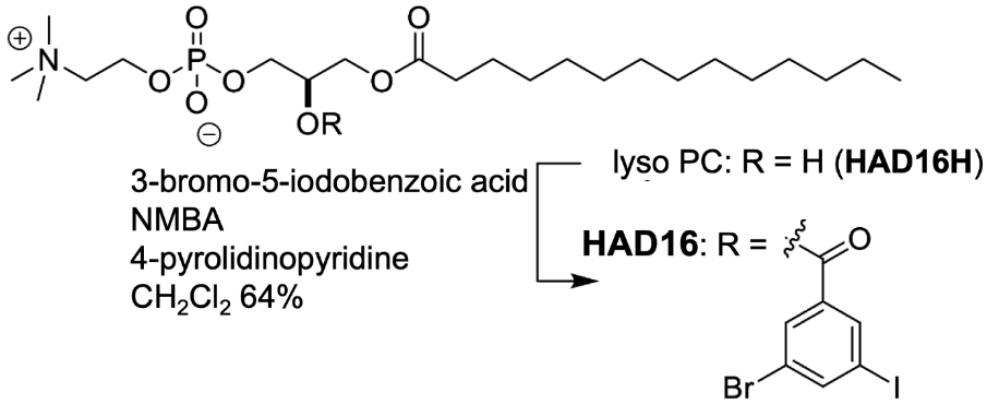

Scheme 4. Synthetic reaction scheme for HAD16. HAD16 was readily produced via a single step synthesis by the esterification. The easy preparation will expand its application range. Details of this synthesis were described in Supplementary Materials.

The HAD16 molecule adopting alternative conformations binds to an interface region among three symmetry-related bacteriorhodopsin molecules (Figure 8). The long alkyl tail of HAD16 interacts with the hydrophobic transmembrane surface. The choline and phosphate group face the bulk solvent. The aromatic ring in the head group ring is stabilized by π–π stacking with Y26 (Figure 8B) and hydrophobic interactions of I/Br atoms with L22, G23, V127, and L221 from a bacteriorhodopsin molecule and W80 from a neighboring molecule. Because a lipid or detergent molecule is located in the corresponding site of the native bacteriorhodopsin structure, we concluded that HAD16 binds to the same site by partially replacing the lipid or detergent. Thus, we modeled lipid/detergent-derived alkyl chains and HAD16 together using partial occupancies. We also collected a dataset from microcrystals soaked with HAD16H lacking the alkyl tail to study the importance of the tail region for bacteriorhodopsin binding (Scheme 4). The anomalous difference map did not show any significant peaks assignable to the compound (data not shown). This establishes that the alkyl chain was indispensable for HAD16 binding to bacteriorhodopsin.

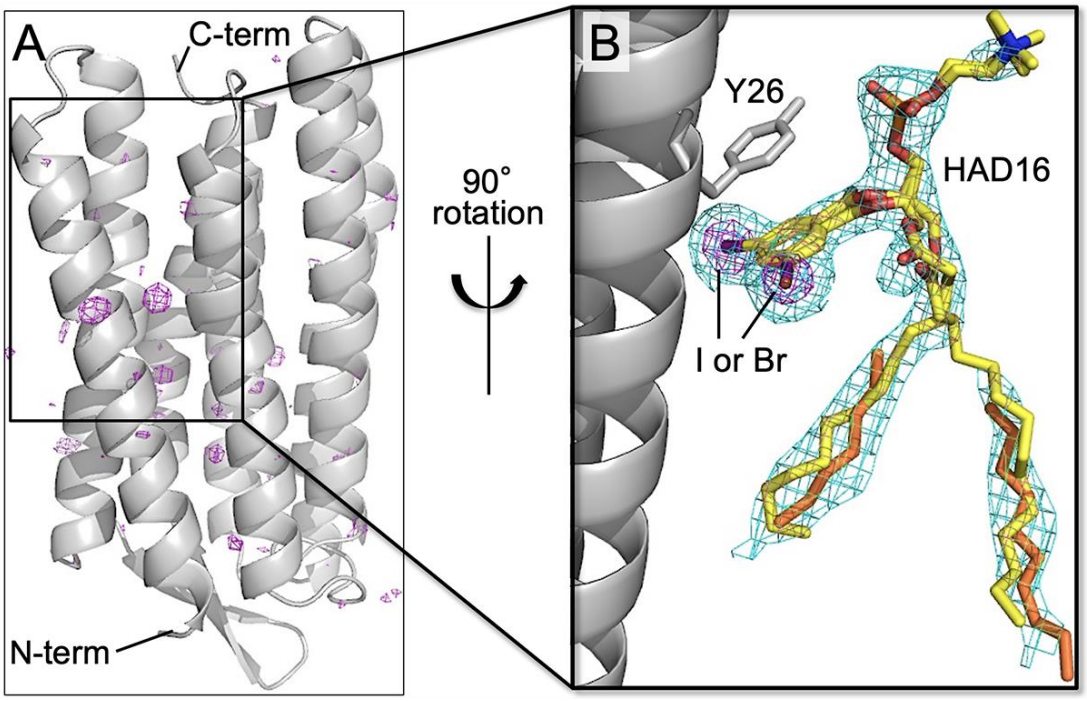

Figure 8. Structure of bacteriorhodopsin in complex with HAD16. (**A**) Final refined structure (gray ribbon model) after structure determination by molecular replacement. Anomalous difference map (purple mesh; contoured at 4.0 σ) is also shown. (**B**) Close-up view of the HAD16 binding site in the final refined structure with 2mF_o–DF_c map (cyan mesh; 1.0 σ). The C, N, O, I, and Br atoms of HAD16 (stick models), which is assigned as alternative conformations, are colored yellow, blue, red, purple, and brown, respectively. Alkyl chains derived from native lipid or DMPC/CHAPSO bicelles are depicted as orange stick models.

4. Conclusions

Biomembranes are the last frontier in life science and the most challenging subject to study. Biomembranes are composed of a lipid bilayer consisting of phospholipids, glycolipids, sterols, and membrane proteins. We presented here artificial lipids and detergents containing heavy atoms, which can be used as components of model biomembranes for analyzing interactions with membrane proteins. In addition to the examples presented above, there is also a study of a detergent labeled with Hg [75]. In combination with X-ray crystallography, these artificial lipids and detergents can be used to determine novel structures of membrane proteins or to identify the orientation of lipid/detergent molecules by visualizing the position of the heavy atoms using anomalous X-ray scattering. In particular, SFX can observe damage-free structures at physiological temperatures. Future applications of these lipids/detergents for elucidating structure–function relationships of membrane proteins and biomembranes include: (i) labeling of various model lipids to distinguish between outer and inner leaflet regions that bind specifically to membrane proteins; (ii) observation of peripheral lipids surrounding membrane proteins with weak affinity at high resolution; and (iii) visualization of the dynamics of lipid localization on the surface of membrane proteins by time-resolved SFX analysis [76].

Supplementary Materials: The following are available online at https://www.mdpi.com/article/10.3390/membranes11110823/s1.

Author Contributions: Conceptualization, S.H. and E.M.; chemical synthesis, S.H.; SFX data analysis, T.N. and E.M.; writing manuscript, S.H. and E.M.; and funding acquisition, S.H. and E.M. All authors have read and agreed to the published version of the manuscript.

Funding: This work was supported by the Japan Science and Technology Agency (JST), PRESTO (JPMJPR17GB), a Grant-in-Aid for Scientific Research on Innovative Areas from the Ministry of Education, Culture, Sports, Science, and Technology (MEXT) (19H05780), a Kakenhi Grant (16H06315)

from Japan Society for the Promotion of Science, the ERATO active lipid structure project from JST, and the X-ray Free Electron Laser Priority Strategy Program of MEXT.

Institutional Review Board Statement: Not applicable.

Informed Consent Statement: Not applicable.

Data Availability Statement: Not applicable.

Acknowledgments: The authors gratefully acknowledge Yo Yano and Haruka Saiki for synthetic efforts and Michio Murata for helpful discussion. We also thank the beamline staff at SACLA for technical assistance and the SACLA High Performance Computing system for computational resource.

Conflicts of Interest: The authors declare no conflict of interest.

Abbreviations

A2A GPCR	G protein-coupled A2a adenosine receptor
α-GalCer	α-galactosylceramide
β-MeSe-Fuc	selenomethyl derivative of fucose
βMeSe-GlcNAc	Selenomethyl-*N*-acetylglucosamine
CHAPSO	3-[(3-cholamidopropyl)dimethylammonio]-2-hydroxypropanesulfonate
CMC	critical micelle concentration
DDM	dodecyl-β-D-maltoside
DMPC	1,2-dimyristoyl-*sn*-glycero-3-phosphocholine
DPPC	dipalmitoylphosphatidylcholine
ERATO	Exploratory Research for Advanced Technology
I3C	5-amino-2,4,6-triiodoisophthalic acid
JST	Japan Science and Technology Agency
LCLS	Linac Coherent Light Source
LCP	lipidic cubic phase
MAD	multi-wavelength anomalous diffraction
MEXT	Ministry of Education, Culture, Sports, Science and Technology
MIR	multiple heavy-atom isomorphous replacement
MIRAS	multiple heavy-atom isomorphous replacement with anomalous scattering
PAL-XFEL	Pohang Accelerator Laboratory X-ray Free Electron Laser
PDB	Protein Data Bank
PRESTO	Precursory Research for Embryonic Science and Technology
SACLA	SPring-8 Angstrom Compact Free Electron Laser
SAD	single-wavelength anomalous diffraction
SeDDM	dodecyl-β-D-selenomaltoside
SFX	serial femtosecond crystallography
SIR	single heavy-atom isomorphous replacement
SIRAS	single heavy-atom isomorphous replacement with anomalous scattering
SRX	synchrotron radiation crystallography
SwissFEL	Swiss X-ray Free Electron Laser
XFEL	X-ray free-electron laser

References

1. Murata, M.; Sugiyama, S.; Matsuoka, S.; Matsumori, N. Bioactive Structure of Membrane Lipids and Natural Products Elucidated by a Chemistry-Based Approach. *Chem. Rec.* **2015**, *15*, 675–690. [CrossRef] [PubMed]
2. Yamashita, T.; Mizohata, E.; Nagatoishi, S.; Watanabe, T.; Nakakido, M.; Iwanari, H.; Mochizuki, Y.; Nakayama, T.; Kado, Y.; Yokota, Y.; et al. Affinity Improvement of a Cancer-Targeted Antibody through Alanine-Induced Adjustment of Antigen-Antibody Interface. *Structure* **2019**, *27*, 519–527.e515. [CrossRef] [PubMed]
3. Nakayama, T.; Mizohata, E.; Yamashita, T.; Nagatoishi, S.; Nakakido, M.; Iwanari, H.; Mochizuki, Y.; Kado, Y.; Yokota, Y.; Satoh, R.; et al. Structural features of interfacial tyrosine residue in ROBO1 fibronectin domain-antibody complex: Crystallographic, thermodynamic, and molecular dynamic analyses. *Protein Sci. A Publ. Protein Soc.* **2015**, *24*, 328–340. [CrossRef] [PubMed]
4. Sugiyama, A.; Kawamura, T.; Tanaka, T.; Doi, H.; Yamashita, T.; Shinoda, K.; Fujitani, H.; Yamatsugu, K.; Shimizu, Y.; Tatsumi, T.; et al. Cupid and Psyche system for the diagnosis and treatment of advanced cancer. *Proc. Jpn. Acad. Ser. B Phys. Biol. Sci.* **2019**, *95*, 602–611. [CrossRef]

5. Kado, Y.; Mizohata, E.; Nagatoishi, S.; Iijima, M.; Shinoda, K.; Miyafusa, T.; Nakayama, T.; Yoshizumi, T.; Sugiyama, A.; Kawamura, T.; et al. Epiregulin recognition mechanisms by anti-epiregulin antibody 9E5: Structural, functional, and molecular dynamics simulation analyses. *J. Biol. Chem.* **2016**, *291*, 2319–2330. [CrossRef]
6. Uchihashi, T.; Ganser, C. Recent advances in bioimaging with high-speed atomic force microscopy. *Biophys. Rev.* **2020**, *12*, 363–369. [CrossRef] [PubMed]
7. Renard, K.; Byrne, B. Insights into the Role of Membrane Lipids in the Structure, Function and Regulation of Integral Membrane Proteins. *Int. J. Mol. Sci.* **2021**, *22*, 9026. [CrossRef] [PubMed]
8. Mizohata, E.; Nakane, T.; Fukuda, Y.; Nango, E.; Iwata, S. Serial femtosecond crystallography at the SACLA: Breakthrough to dynamic structural biology. *Biophys. Rev.* **2018**, *10*, 209–218. [CrossRef] [PubMed]
9. Hendrickson, W.A.; Teeter, M.M. Structure of the Hydrophobic Protein Crambin Determined Directly from the Anomalous Scattering of Sulfur. *Nature* **1981**, *290*, 107–113. [CrossRef]
10. Agniswamy, J.; Joyce, M.G.; Hammer, C.H.; Sun, P.D. Towards a rational approach for heavy-atom derivative screening in protein crystallography. *Acta Crystallogr. Sect. D Biol. Crystallogr.* **2008**, *64*, 354–367. [CrossRef]
11. Lu, J.; Sun, P.D. A rapid and rational approach to generating isomorphous heavy-atom phasing derivatives. *FEBS J.* **2014**, *281*, 4021–4028. [CrossRef]
12. Allen, F.H.K.O.; Watson, D.G.; Brammer, L.; Orpen, A.G.; Taylor, R. Tables of bond lengths determined by x-ray and neutron diffraction. Part 1. Bond lengths in organic compounds. *J. Chem. Soc. Perkin Trans.* **1987**, *2*, 1–19. [CrossRef]
13. Blanksby, S.J.; Ellison, G.B. Bond dissociation energies of organic molecules. *Acc. Chem. Res.* **2003**, *36*, 255–263. [CrossRef] [PubMed]
14. Dong, Y.Y.; Pike, A.C.; Mackenzie, A.; McClenaghan, C.; Aryal, P.; Dong, L.; Quigley, A.; Grieben, M.; Goubin, S.; Mukhopadhyay, S.; et al. K2P channel gating mechanisms revealed by structures of TREK-2 and a complex with Prozac. *Science* **2015**, *347*, 1256–1259. [CrossRef]
15. Ulens, C.; Spurny, R.; Thompson, A.J.; Alqazzaz, M.; Debaveye, S.; Han, L.; Price, K.; Villalgordo, J.M.; Tresadern, G.; Lynch, J.W.; et al. The prokaryote ligand-gated ion channel ELIC captured in a pore blocker-bound conformation by the Alzheimer's disease drug memantine. *Structure* **2014**, *22*, 1399–1407. [CrossRef] [PubMed]
16. Martick, M.; Scott, W.G. Tertiary contacts distant from the active site prime a ribozyme for catalysis. *Cell* **2006**, *126*, 309–320. [CrossRef]
17. Stagno, J.R.; Yu, P.; Dyba, M.A.; Wang, Y.X.; Liu, Y. Heavy-atom labeling of RNA by PLOR for de novo crystallographic phasing. *PLoS ONE* **2019**, *14*, e0215555. [CrossRef]
18. Czapinska, H.; Winiewska-Szajewska, M.; Szymaniec-Rutkowska, A.; Piasecka, A.; Bochtler, M.; Poznanski, J. Halogen Atoms in the Protein-Ligand System. Structural and Thermodynamic Studies of the Binding of Bromobenzotriazoles by the Catalytic Subunit of Human Protein Kinase CK2. *J. Phys. Chem. B* **2021**, *125*, 2491–2503. [CrossRef]
19. Scholfield, M.R.; Zanden, C.M.; Carter, M.; Ho, P.S. Halogen bonding (X-bonding): A biological perspective. *Protein Sci. A Publ. Protein Soc.* **2013**, *22*, 139–152. [CrossRef]
20. Silvius, J.R. Cholesterol modulation of lipid intermixing in phospholipid and glycosphingolipid mixtures. Evaluation using fluorescent lipid probes and brominated lipid quenchers. *Biochemistry* **1992**, *31*, 3398–3408. [CrossRef]
21. Abrams, F.S.; London, E. Calibration of the parallax fluorescence quenching method for determination of membrane penetration depth: Refinement and comparison of quenching by spin-labeled and brominated lipids. *Biochemistry* **1992**, *31*, 5312–5322. [CrossRef] [PubMed]
22. Bolen, E.J.; Holloway, P.W. Quenching of tryptophan fluorescence by brominated phospholipid. *Biochemistry* **1990**, *29*, 9638–9643. [CrossRef]
23. Halter, M.; Nogata, Y.; Dannenberger, O.; Sasaki, T.; Vogel, V. Engineered lipids that cross-link the inner and outer leaflets of lipid bilayers. *Langmuir* **2004**, *20*, 2416–2423. [CrossRef] [PubMed]
24. Markello, T.; Zlotnick, A.; Everett, J.; Tennyson, J.; Holloway, P.W. Determination of the topography of cytochrome b5 in lipid vesicles by fluorescence quenching. *Biochemistry* **1985**, *24*, 2895–2901. [CrossRef]
25. Cudmore, A.J.; Bradshaw, J.P.; Alecio, M.R. X-Ray-Diffraction Studies Using a Novel Synthetic Phospholipid. *Biophys. Chem.* **1994**, *49*, 71–76. [CrossRef]
26. Roszak, A.W.; Gardiner, A.T.; Isaacs, N.W.; Cogdell, R.J. Brominated lipids identify lipid binding sites on the surface of the reaction center from Rhodobacter sphaeroides. *Biochemistry* **2007**, *46*, 2909–2916. [CrossRef] [PubMed]
27. Campanacci, V.; Lartigue, A.; Hallberg, B.M.; Jones, T.A.; Giudici-Orticoni, M.T.; Tegoni, M.; Cambillau, C. Moth chemosensory protein exhibits drastic conformational changes and cooperativity on ligand binding. *Proc. Natl. Acad. Sci. USA* **2003**, *100*, 5069–5074. [CrossRef]
28. Lautenschlager, C.; Leal, W.S.; Clardy, J. Bombyx mori pheromone-binding protein binding nonpheromone ligands: Implications for pheromone recognition. *Structure* **2007**, *15*, 1148–1154. [CrossRef] [PubMed]
29. Chae, P.S.C.; Cho, K.H.; Bae, H.E. Heavy atom-bearing tripod amphiphiles for the membrane protein study. *New J. Chem.* **2014**, *38*, 2354–2361. [CrossRef]
30. Beck, T.; Krasauskas, A.; Gruene, T.; Sheldrick, G.M. A magic triangle for experimental phasing of macromolecules. *Acta Crystallogr. Sect. D Biol. Crystallogr.* **2008**, *64*, 1179–1182. [CrossRef]

31. Sippel, K.H.; Robbins, A.H.; Reutzel, R.; Domsic, J.; Boehlein, S.K.; Govindasamy, L.; Agbandje-McKenna, M.; Rosser, C.J.; McKenna, R. Structure determination of the cancer-associated Mycoplasma hyorhinis protein Mh-p37. *Acta Crystallogr. Sect. D Biol. Crystallogr.* **2008**, *64*, 1172–1178. [CrossRef] [PubMed]
32. Nakane, T.; Hanashima, S.; Suzuki, M.; Saiki, H.; Hayashi, T.; Kakinouchi, K.; Sugiyama, S.; Kawatake, S.; Matsuoka, S.; Matsumori, N.; et al. Membrane protein structure determination by SAD, SIR, or SIRAS phasing in serial femtosecond crystallography using an iododetergent. *Proc. Natl. Acad. Sci. USA* **2016**, *113*, 13039–13044. [CrossRef]
33. Katzberg, R.W. Urography into the 21st century: New contrast media, renal handling, imaging characteristics, and nephrotoxicity. *Radiology* **1997**, *204*, 297–312. [CrossRef] [PubMed]
34. Yu, S.B.; Watson, A.D. Metal-Based X-ray Contrast Media. *Chem. Rev.* **1999**, *99*, 2353–2378. [CrossRef]
35. Beck, T.; Gruene, T.; Sheldrick, G.M. The magic triangle goes MAD: Experimental phasing with a bromine derivative. *Acta Crystallogr. Sect. D Biol. Crystallogr.* **2010**, *66*, 374–380. [CrossRef] [PubMed]
36. Truong, J.Q.; Nguyen, S.; Bruning, J.B.; Shearwin, K.E. Simplified heavy-atom derivatization of protein structures via co-crystallization with the MAD tetragon tetrabromoterephthalic acid. *Acta Cryst. F Struct. Biol. Commun.* **2021**, *77*, 156–162. [CrossRef]
37. Faham, S.; Boulting, G.L.; Massey, E.A.; Yohannan, S.; Yang, D.; Bowie, J.U. Crystallization of bacteriorhodopsin from bicelle formulations at room temperature. *Protein Sci. A Publ. Protein Soc.* **2005**, *14*, 836–840. [CrossRef] [PubMed]
38. Hendrickson, W.A.; Horton, J.R.; LeMaster, D.M. Selenomethionyl proteins produced for analysis by multiwavelength anomalous diffraction (MAD): A vehicle for direct determination of three-dimensional structure. *EMBO J.* **1990**, *9*, 1665–1672. [CrossRef]
39. Lin, L.; Sheng, J.; Huang, Z. Nucleic acid X-ray crystallography via direct selenium derivatization. *Chem. Soc. Rev.* **2011**, *40*, 4591–4602. [CrossRef] [PubMed]
40. Merino-Montiel, P.L.; López, Ó.; Fernández-Bolaños, J.G. L-Isofucoselenofagomine and derivatives: Dual activities as antioxidants and as glycosidase inhibitors. *Tetrahedron* **2012**, *68*, 3591–3595. [CrossRef]
41. Mangiavacchi, F.; Coelho Dias, I.F.; Di Lorenzo, I.; Grzes, P.; Palomba, M.; Rosati, O.; Bagnoli, L.; Marini, F.; Santi, C.; Lenardao, E.J.; et al. Sweet Selenium: Synthesis and Properties of Selenium-Containing Sugars and Derivatives. *Pharmaceuticals* **2020**, *13*. [CrossRef]
42. Davies, M.J.S.; Schiesser, C.H. 1,4-Anhydro-4-seleno-d-talitol (SeTal): A remarkable selenium-containing therapeutic molecule. *New J. Chem.* **2019**, *43*, 9759–9765. [CrossRef]
43. Buts, L.; Loris, R.; De Genst, E.; Oscarson, S.; Lahmann, M.; Messens, J.; Brosens, E.; Wyns, L.; De Greve, H.; Bouckaert, J. Solving the phase problem for carbohydrate-binding proteins using selenium derivatives of their ligands: A case study involving the bacterial F17-G adhesin. *Acta Crystallogr. Sect. D Biol. Crystallogr.* **2003**, *59*, 1012–1015. [CrossRef]
44. Kostlanova, N.; Mitchell, E.P.; Lortat-Jacob, H.; Oscarson, S.; Lahmann, M.; Gilboa-Garber, N.; Chambat, G.; Wimmerova, M.; Imberty, A. The fucose-binding lectin from Ralstonia solanacearum. A new type of beta-propeller architecture formed by oligomerization and interacting with fucoside, fucosyllactose, and plant xyloglucan. *J. Biol. Chem.* **2005**, *280*, 27839–27849. [CrossRef] [PubMed]
45. Houser, J.; Komarek, J.; Kostlanova, N.; Cioci, G.; Varrot, A.; Kerr, S.C.; Lahmann, M.; Balloy, V.; Fahy, J.V.; Chignard, M.; et al. A soluble fucose-specific lectin from Aspergillus fumigatus conidia–structure, specificity and possible role in fungal pathogenicity. *PLoS ONE* **2013**, *8*, e83077. [CrossRef] [PubMed]
46. Sulak, O.; Cioci, G.; Delia, M.; Lahmann, M.; Varrot, A.; Imberty, A.; Wimmerova, M. A TNF-like trimeric lectin domain from Burkholderia cenocepacia with specificity for fucosylated human histo-blood group antigens. *Structure* **2010**, *18*, 59–72. [CrossRef] [PubMed]
47. Sommer, R.; Hauck, D.; Varrot, A.; Imberty, A.; Kunzler, M.; Titz, A. O-Alkylated heavy atom carbohydrate probes for protein X-ray crystallography: Studies towards the synthesis of methyl 2-O-methyl-L-selenofucopyranoside. *Beilstein. J. Org. Chem.* **2016**, *12*, 2828–2833. [CrossRef] [PubMed]
48. Shimabukuro, J.; Makyio, H.; Suzuki, T.; Nishikawa, Y.; Kawasaki, M.; Imamura, A.; Ishida, H.; Ando, H.; Kato, R.; Kiso, M. Synthesis of seleno-fucose compounds and their application to the X-ray structural determination of carbohydrate-lectin complexes using single/multi-wavelength anomalous dispersion phasing. *Bioorg. Med. Chem.* **2017**, *25*, 1132–1142. [CrossRef] [PubMed]
49. Makyio, H.; Shimabukuro, J.; Suzuki, T.; Imamura, A.; Ishida, H.; Kiso, M.; Ando, H.; Kato, R. Six independent fucose-binding sites in the crystal structure of Aspergillus oryzae lectin. *Biochem. Biophys. Res. Commun.* **2016**, *477*, 477–482. [CrossRef]
50. Suzuki, T.; Hayashi, C.; Komura, N.; Tamai, R.; Uzawa, J.; Ogawa, J.; Tanaka, H.N.; Imamura, A.; Ishida, H.; Kiso, M.; et al. Synthesis and Glycan-Protein Interaction Studies of Se-Sialosides by (77)Se NMR. *Org. Lett.* **2019**, *21*, 6393–6396. [CrossRef] [PubMed]
51. Saino, H.; Ago, H.; Ukita, Y.; Miyano, M. Seleno-detergent MAD phasing of leukotriene C4 synthase in complex with dodecyl-beta-D-selenomaltoside. *Acta Crystallogr. Sect. F Struct. Biol. Cryst. Commun.* **2011**, *67*, 1666–1673. [CrossRef] [PubMed]
52. Sauguet, L.; Poitevin, F.; Murail, S.; Van Renterghem, C.; Moraga-Cid, G.; Malherbe, L.; Thompson, A.W.; Koehl, P.; Corringer, P.J.; Baaden, M.; et al. Structural basis for ion permeation mechanism in pentameric ligand-gated ion channels. *EMBO J.* **2013**, *32*, 728–741. [CrossRef] [PubMed]
53. Fredga, A.L.; Lindgren, A. Selena-hexanoic and Selena-pentanoic Acids. *Acta Chem. Scand.* **1961**, *15*, 938–939. [CrossRef]

54. Golmohammadi, R. Studies on the methods of preparation of di- and tri-selena-straight-chain fatty acids and corresponding amides, with some remarks on the infrared spectra of the mono-, di- and tri-selena-fatty acids. *Acta Chem. Scand.* **1966**, *20*, 563–571. [CrossRef]
55. Sadek, S.A.B.; Basmadjian, G.P. Selenium labeled fatty acids as potential myocardial imaging agents. *J. Label. Compd. Radiopharm.* **1983**, *20*, 487–494. [CrossRef]
56. Yanishlieva, N.R.; Marinova, E.; Houte, H.; Partali, V.; Sliwka, H.R. 11-Selenadodecylglyceryl-1-ether in lipid autoxidation. *J. Am. Oil Chem. Soc.* **2001**, *78*, 691–696. [CrossRef]
57. Houte, H.; Partali, V.; Sliwka, H.R.; Quartey, E.G. Synthesis of structured lipids and etherlipids with antioxidants: Combination of a selena fatty acid and a selena fatty alcohol with a carotenoic acid in glyceride molecules. *Chem. Phys. Lipids* **2000**, *105*, 105–113. [CrossRef]
58. Kabara, J.J.; Vrable, R. Antimicrobial lipids: Natural and synthetic fatty acids and monoglycerides. *Lipids* **1977**, *12*, 753–759. [CrossRef] [PubMed]
59. Hossain, M.I.; Hanashima, S.; Nomura, T.; Lethu, S.; Tsuchikawa, H.; Murata, M.; Kusaka, H.; Kita, S.; Maenaka, K. Synthesis and Th1-immunostimulatory activity of alpha-galactosylceramide analogues bearing a halogen-containing or selenium-containing acyl chain. *Bioorg. Med. Chem.* **2016**, *24*, 3687–3695. [CrossRef] [PubMed]
60. Emma, P.; Akre, R.; Arthur, J.; Bionta, R.; Bostedt, C.; Bozek, J.; Brachmann, A.; Bucksbaum, P.; Coffee, R.; Decker, F.J.; et al. First lasing and operation of an angstrom-wavelength free-electron laser. *Nat. Photonics* **2010**, *4*, 641–647. [CrossRef]
61. Ishikawa, T.; Aoyagi, H.; Asaka, T.; Asano, Y.; Azumi, N.; Bizen, T.; Ego, H.; Fukami, K.; Fukui, T.; Furukawa, Y.; et al. A compact X-ray free-electron laser emitting in the sub-angstrom region. *Nat. Photonics* **2012**, *6*, 540–544. [CrossRef]
62. Decking, W.; Abeghyan, S.; Abramian, P.; Abramsky, A.; Aguirre, A.; Albrecht, C.; Alou, P.; Altarelli, M.; Altmann, P.; Amyan, K.; et al. A MHz-repetition-rate hard X-ray free-electron laser driven by a superconducting linear accelerator. *Nat. Photonics* **2020**, *14*, 391–397. [CrossRef]
63. Kang, H.S.; Min, C.K.; Heo, H.; Kim, C.; Yang, H.; Kim, G.; Nam, I.; Baek, S.Y.; Choi, H.J.; Mun, G.; et al. Hard X-ray free-electron laser with femtosecond-scale timing jitter. *Nat. Photonics* **2017**, *11*, 708–713. [CrossRef]
64. Prat, E.; Abela, R.; Aiba, M.; Alarcon, A.; Alex, J.; Arbelo, Y.; Arrell, C.; Arsov, V.; Bacellar, C.; Beard, C.; et al. A compact and cost-effective hard X-ray free-electron laser driven by a high-brightness and low-energy electron beam. *Nat. Photonics* **2020**, *14*, 748–754. [CrossRef]
65. Chapman, H.N.; Fromme, P.; Barty, A.; White, T.A.; Kirian, R.A.; Aquila, A.; Hunter, M.S.; Schulz, J.; DePonte, D.P.; Weierstall, U.; et al. Femtosecond X-ray protein nanocrystallography. *Nature* **2011**, *470*, 73–77. [CrossRef] [PubMed]
66. Tono, K.; Nango, E.; Sugahara, M.; Song, C.; Park, J.; Tanaka, T.; Tanaka, R.; Joti, Y.; Kameshima, T.; Ono, S.; et al. Diverse application platform for hard X-ray diffraction in SACLA (DAPHNIS): Application to serial protein crystallography using an X-ray free-electron laser. *J. Synchrotron Radiat.* **2015**, *22*, 532–537. [CrossRef]
67. Fukuda, Y.; Tse, K.M.; Nakane, T.; Nakatsu, T.; Suzuki, M.; Sugahara, M.; Inoue, S.; Masuda, T.; Yumoto, F.; Matsugaki, N.; et al. Redox-coupled proton transfer mechanism in nitrite reductase revealed by femtosecond crystallography. *Proc. Natl. Acad. Sci. USA* **2016**, *113*, 2928–2933. [CrossRef]
68. Barty, A.; Caleman, C.; Aquila, A.; Timneanu, N.; Lomb, L.; White, T.A.; Andreasson, J.; Arnlund, D.; Bajt, S.; Barends, T.R.; et al. Self-terminating diffraction gates femtosecond X-ray nanocrystallography measurements. *Nat. Photonics* **2012**, *6*, 35–40. [CrossRef] [PubMed]
69. Barends, T.R.; Foucar, L.; Botha, S.; Doak, R.B.; Shoeman, R.L.; Nass, K.; Koglin, J.E.; Williams, G.J.; Boutet, S.; Messerschmidt, M.; et al. De novo protein crystal structure determination from X-ray free-electron laser data. *Nature* **2014**, *505*, 244–247. [CrossRef] [PubMed]
70. Yamashita, K.; Pan, D.; Okuda, T.; Sugahara, M.; Kodan, A.; Yamaguchi, T.; Murai, T.; Gomi, K.; Kajiyama, N.; Mizohata, E.; et al. An isomorphous replacement method for efficient de novo phasing for serial femtosecond crystallography. *Sci. Rep.* **2015**, *5*, 14017. [CrossRef] [PubMed]
71. Nakane, T.; Song, C.; Suzuki, M.; Nango, E.; Kobayashi, J.; Masuda, T.; Inoue, S.; Mizohata, E.; Nakatsu, T.; Tanaka, T.; et al. Native sulfur/chlorine SAD phasing for serial femtosecond crystallography. *Acta Crystallogr. Sect. D Biol. Crystallogr.* **2015**, *71*, 2519–2525. [CrossRef] [PubMed]
72. Colletier, J.P.; Sawaya, M.R.; Gingery, M.; Rodriguez, J.A.; Cascio, D.; Brewster, A.S.; Michels-Clark, T.; Hice, R.H.; Coquelle, N.; Boutet, S.; et al. De novo phasing with X-ray laser reveals mosquito larvicide BinAB structure. *Nature* **2016**, *539*, 43–47. [CrossRef] [PubMed]
73. Hunter, M.S.; Yoon, C.H.; DeMirci, H.; Sierra, R.G.; Dao, E.H.; Ahmadi, R.; Aksit, F.; Aquila, A.L.; Ciftci, H.; Guillet, S.; et al. Selenium single-wavelength anomalous diffraction de novo phasing using an X-ray-free electron laser. *Nat. Commun.* **2016**, *7*. [CrossRef]
74. Batyuk, A.; Galli, L.; Ishchenko, A.; Han, G.W.; Gati, C.; Popov, P.A.; Lee, M.Y.; Stauch, B.; White, T.A.; Barty, A.; et al. Native phasing of x-ray free-electron laser data for a G protein-coupled receptor. *Sci. Adv.* **2016**, *2*, e1600292. [CrossRef] [PubMed]
75. Cogdell, R.J.; Gardiner, A.T.; Roszak, A.W.; Stoncius, S.; Kocovsky, P.; Isaacs, N.W. Mapping lipid and detergent molecules at the surface of membrane proteins. *Biochem. Soc. Trans.* **2011**, *39*, 775–779. [CrossRef] [PubMed]
76. Nango, E.; Royant, A.; Kubo, M.; Nakane, T.; Wickstrand, C.; Kimura, T.; Tanaka, T.; Tono, K.; Song, C.; Tanaka, R.; et al. A three-dimensional movie of structural changes in bacteriorhodopsin. *Science* **2016**, *354*, 1552–1557. [CrossRef]